

Beyond MLE and GLRT

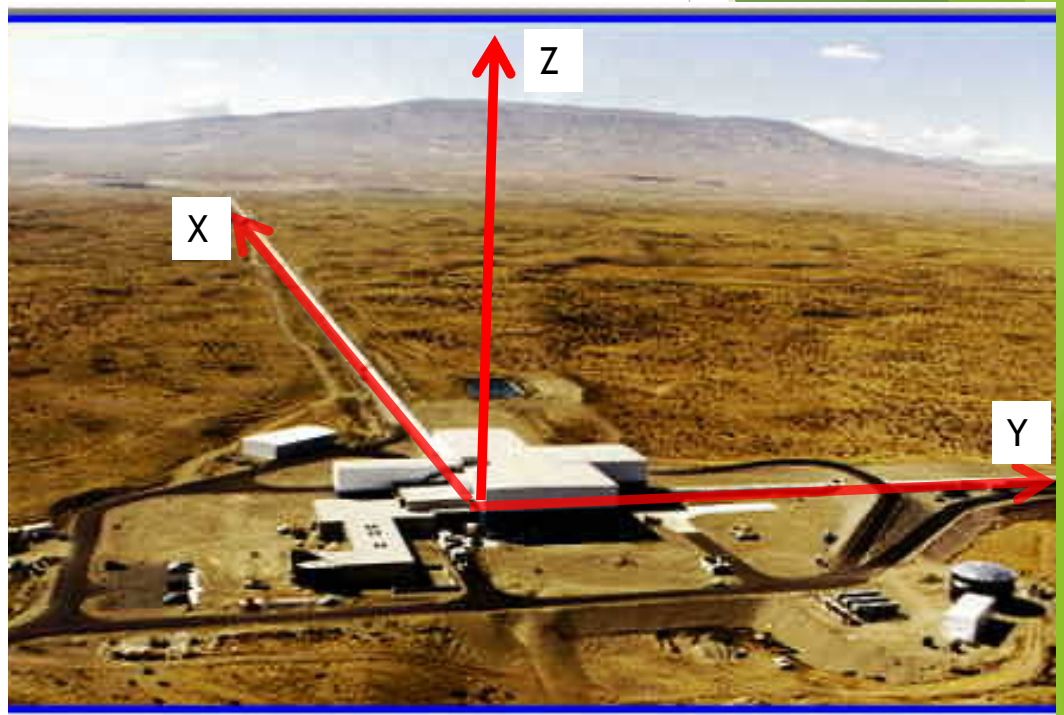
SIGNAL MODELS

- MLE and GLRT both require reliable **signal models**
- Many anticipated GW sources do not have reliable signal models, for example:
 - Core-collapse supernova signals for ground-based detectors: turbulent dynamics → fundamentally unpredictable waveforms
 - Extreme mass ratio inspiral signals for LISA: two-body problem in GR but very challenging to compute accurately
- It is possible to extend MLE and GLRT to the case of where signal models are not known:
Requires **regularization techniques**
 - Various types of time-frequency analysis methods may also be used
- MLE and GLRT also require reliable **noise models**
- Data analysis techniques (e.g., **veto**) are needed to bring the performance of MLE and GLRT closer to the ideal one

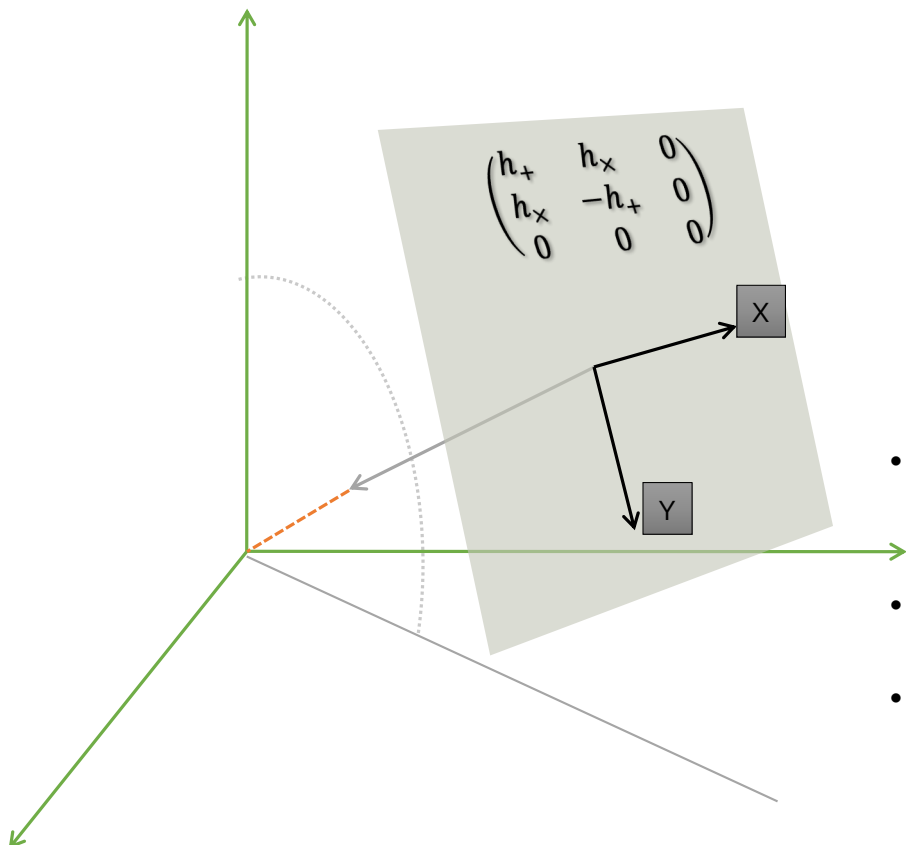
REGULARIZATION

Strain signal

- ▶ GW interferometer: Measured quantity is the difference in arm lengths
- ▶ Detector tensor:
$$\vec{D} = \hat{n}_X \otimes \hat{n}_X - \hat{n}_Y \otimes \hat{n}_Y$$
- ▶ Defined purely by the orientation of the detector arms
- ▶ Strain signal:
$$s(t) = \overleftrightarrow{W} : \vec{D}$$



Wave tensor



- The wave tensor is expressed most simply in the “Wave frame”: Z-axis along wave propagation direction
- In terms of X and Y axes orthogonal to wave frame Z-axis:

$$\begin{pmatrix} h_+ & h_x & 0 \\ h_x & -h_+ & 0 \\ 0 & 0 & 0 \end{pmatrix} = h_+(t) \begin{pmatrix} 1 & 0 & 0 \\ 0 & -1 & 0 \\ 0 & 0 & 0 \end{pmatrix} + h_x(t) \begin{pmatrix} 0 & 1 & 0 \\ 1 & 0 & 0 \\ 0 & 0 & 0 \end{pmatrix}$$

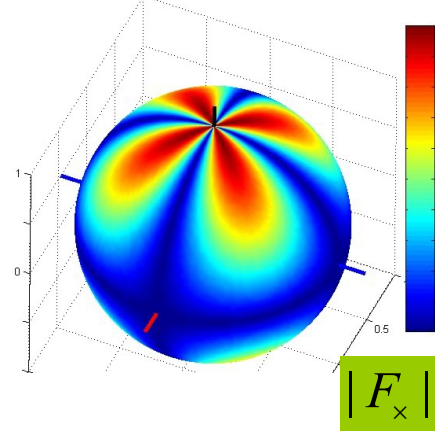
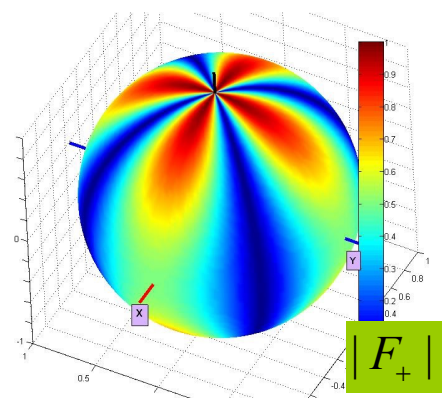
$$\overleftrightarrow{W} = \frac{1}{2}h_+(t)(\hat{x}\otimes\hat{x} - \hat{y}\otimes\hat{y}) + \frac{1}{2}h_x(t)(\hat{x}\otimes\hat{y} + \hat{y}\otimes\hat{x})$$

- Common notation in papers:
- $\overleftrightarrow{W} = h_+(t)\overleftrightarrow{e}_+ + h_x(t)\overleftrightarrow{e}_x$
- \overleftrightarrow{e}_+ and \overleftrightarrow{e}_x are called “plus” and “cross” polarization tensors
 - The wave tensor is defined purely in terms of the wave frame

GW strain signal

$$s(t) = \vec{W} \cdot \vec{D} = h_+(t) \vec{e}_+(\hat{n}) \cdot \vec{D} + h_x(t) \vec{e}_x(\hat{n}) \cdot \vec{D} = h_+(t) F_+(\hat{n}) + h_x(t) F_x(\hat{n})$$

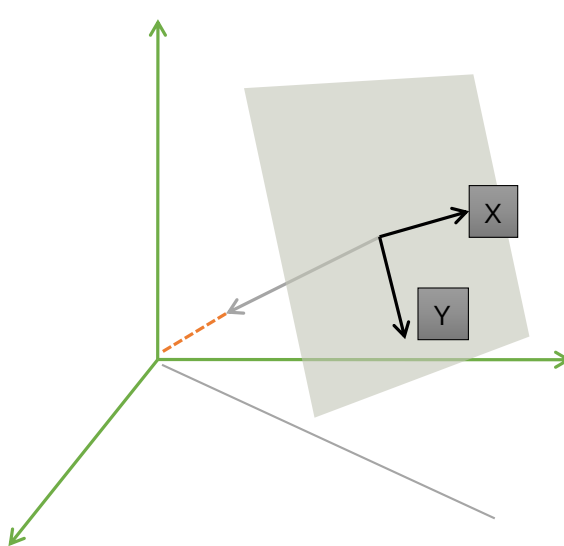
- $F_{+,x}$ are called the **antenna pattern functions** of the detector and depend on the direction \hat{n} to the GW source



Wave frame conventions

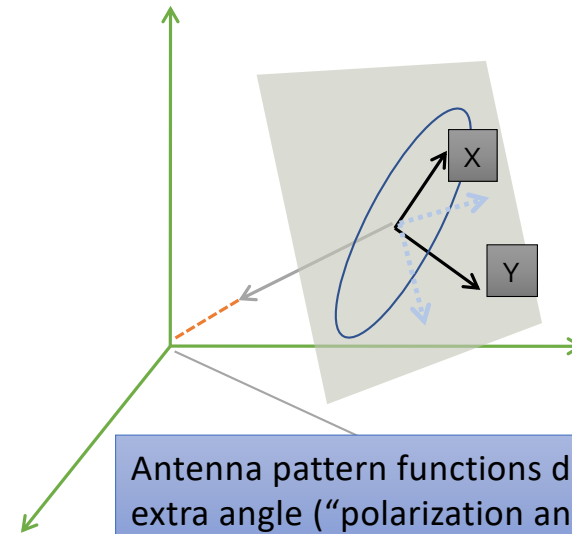
Burst signals

- Fix the wave frame XY axes by convention



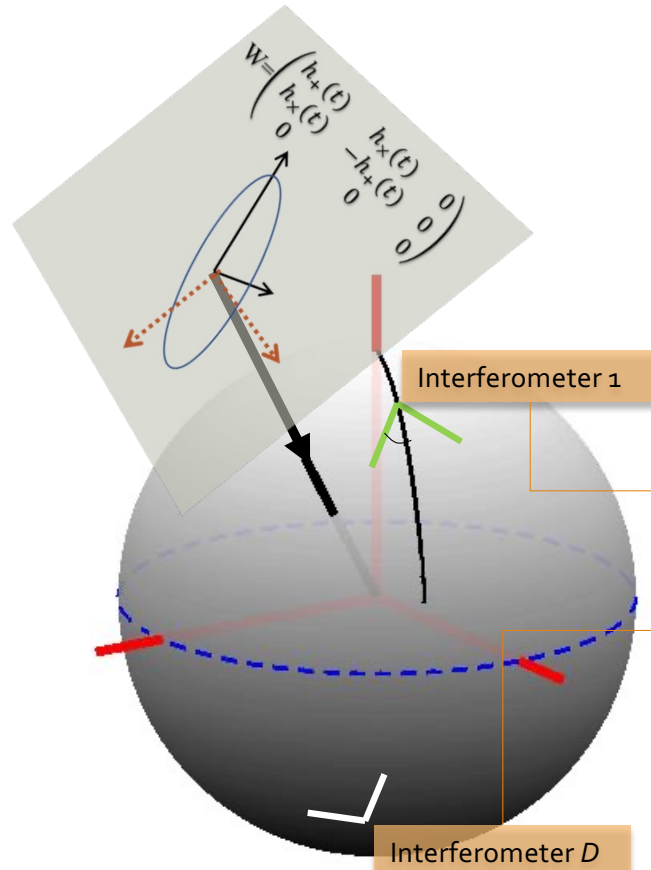
Inspiral signals

- Fix the wave frame XY axes according to binary orbit projected on the sky

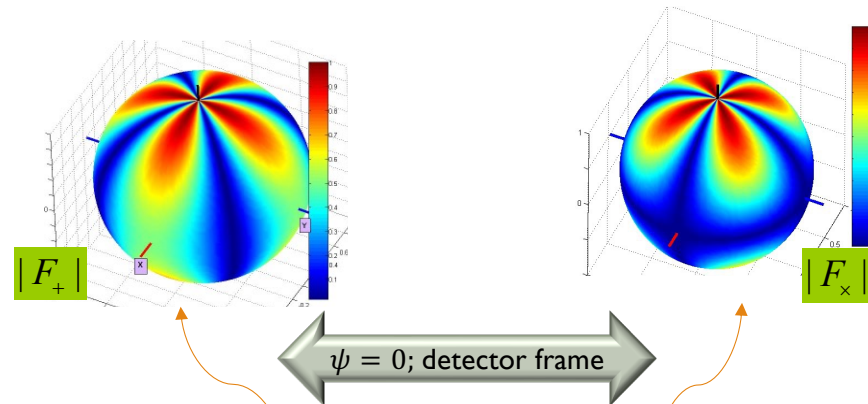


Antenna pattern functions depend on
extra angle (“polarization angle”): ψ

NETWORK RESPONSE



CENTRA, Technical University of Lisbon



$$\begin{pmatrix} s_1(t) \\ s_2(t) \\ \vdots \\ s_D(t) \end{pmatrix} = \begin{pmatrix} F_{+,1}(\hat{n}, \psi) \mathbf{T}[\tau_1(\hat{n})] & F_{x,1}(\hat{n}, \psi) \mathbf{T}[\tau_1(\hat{n})] \\ F_{+,2}(\hat{n}, \psi) \mathbf{T}[\tau_2(\hat{n})] & F_{x,2}(\hat{n}, \psi) \mathbf{T}[\tau_2(\hat{n})] \\ \vdots & \vdots \\ F_{+,D}(\hat{n}, \psi) \mathbf{T}[\tau_D(\hat{n})] & F_{x,D}(\hat{n}, \psi) \mathbf{T}[\tau_D(\hat{n})] \end{pmatrix} \begin{pmatrix} h_+(t; \Theta) \\ h_x(t; \Theta) \end{pmatrix}$$

\hat{n} : Unit vector pointing to GW source from geocenter

ψ : Orientation of preferred wave-frame w.r.t to geocentric wave-frame

Θ : Other parameters of the signal such as: time of arrival, amplitude, initial phase, component masses, spins, ...

$\mathbf{T}[\tau]f(t) = f(t - \tau)$: Time-delay w.r.t geocenter

NETWORK DATA: BURST SIGNALS

$$\begin{pmatrix} y_1(t) \\ y_2(t) \\ \vdots \\ y_D(t) \end{pmatrix} = \begin{pmatrix} F_{+,1}(\hat{n})\mathbf{T}[\tau_1(\hat{n})] & F_{x,1}(\hat{n})\mathbf{T}[\tau_1(\hat{n})] \\ F_{+,2}(\hat{n})\mathbf{T}[\tau_2(\hat{n})] & F_{x,2}(\hat{n})\mathbf{T}[\tau_2(\hat{n})] \\ \vdots & \vdots \\ F_{+,D}(\hat{n})\mathbf{T}[\tau_D(\hat{n})] & F_{x,D}(\hat{n})\mathbf{T}[\tau_D(\hat{n})] \end{pmatrix} \begin{pmatrix} h_+(t; \Theta) \\ h_x(t; \Theta) \end{pmatrix} + \begin{pmatrix} n_1(t) \\ n_2(t) \\ \vdots \\ n_D(t) \end{pmatrix}$$

GW detector data

Noise

$$\mathbf{y}(t) = \mathbf{A}(\hat{n})\mathbf{h}(t) + \mathbf{n}(t)$$

Treat each sample value of
 $\mathbf{h}(t)$ as an extrinsic parameter

$$\begin{aligned} \mathbf{h}_{MLE}(t) &= \mathbf{M} \mathbf{A}^T(\hat{n}_{MLE}) \mathbf{y}(t) \\ \mathbf{M} &= (\mathbf{A}^T(\hat{n}_{MLE}) \mathbf{A}(\hat{n}_{MLE}))^{-1} \end{aligned}$$

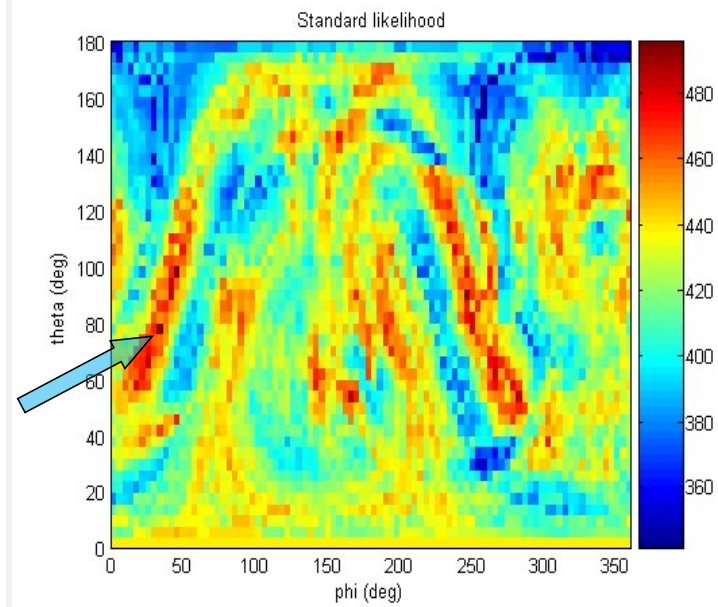
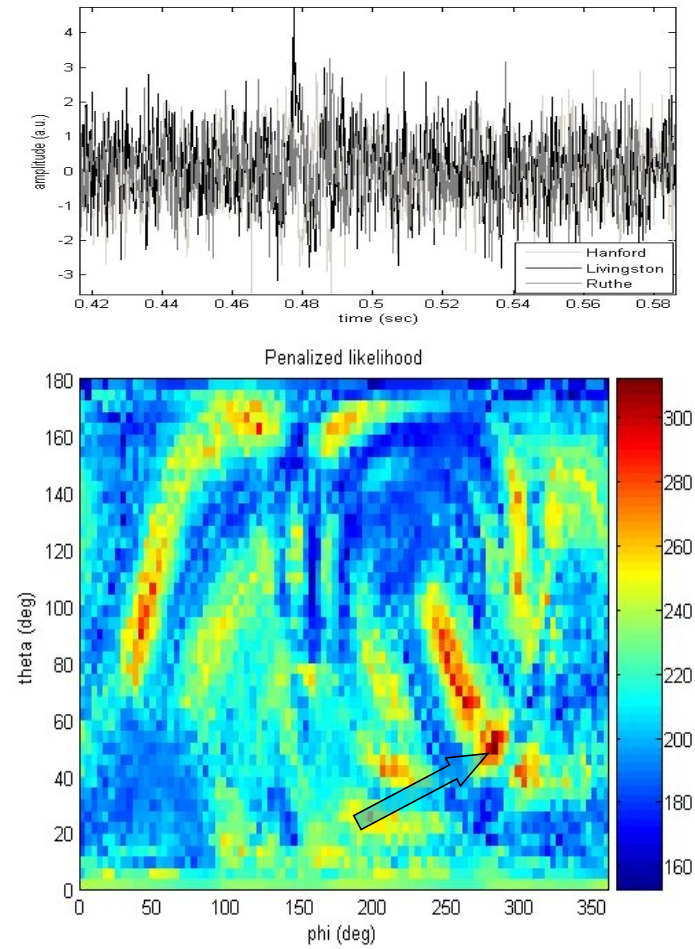
But the problem is *ill-posed!* $\mathbf{A}(\hat{n})$ can become *rank-deficient*
 ⇒ Noise in $\mathbf{y}(t)$ is greatly magnified and creates large errors in the MLE parameter estimates $\mathbf{h}_{MLE}(t)$ and \hat{n}_{MLE}

REGULARIZATION: CHANGING THE FITNESS FUNCTION

$$\max_{\bar{h}} \|\bar{y} - A(\hat{n}) \bar{h}\|^2 \rightarrow \max_{\bar{h}} \left[\|\bar{y} - A(\hat{n}) \bar{h}\|^2 + \underbrace{\lambda P(\bar{h})}_{Regulator} \right]$$

- The regulator pushes the solution towards a more desirable one that is less sensitive to noise and ill-posedness
 - Klimenko, Mohanty, Rakhmanov, Mitselmakher, PRD, 2005 → Basis of the current main analysis pipeline – Coherent Wave Burst (CWb) -- for burst signals in LIGO
 - Mohanty, Rakhmanov, Klimenko, Mitselmakher, CQG, 2006

REGULARIZED MLE DEMO: LIGO AND GEO600

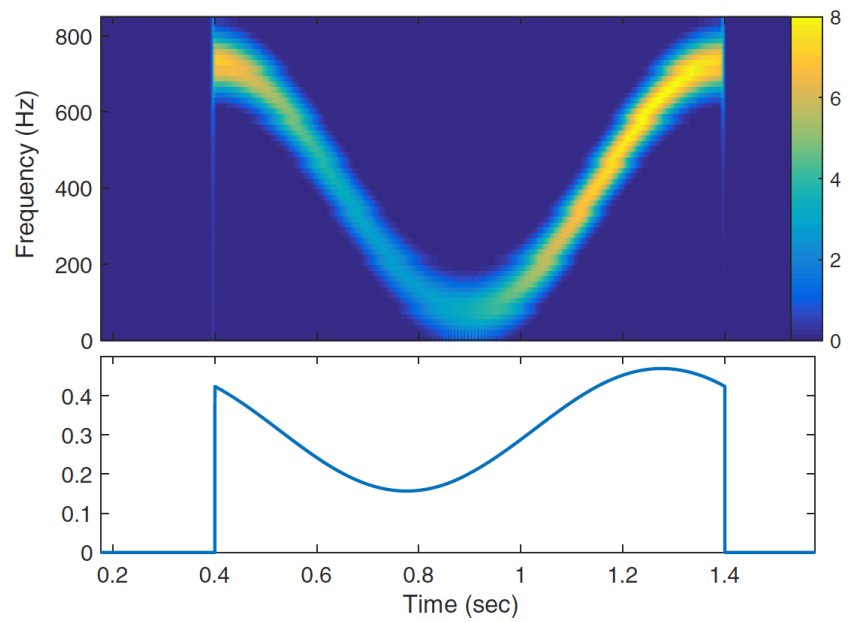


- Likelihood of source at sky angles (θ, φ)
- Without regulator, the source location has a large error
- Regulator introduces a small bias but drastically reduces the variance

Unmodeled chirps

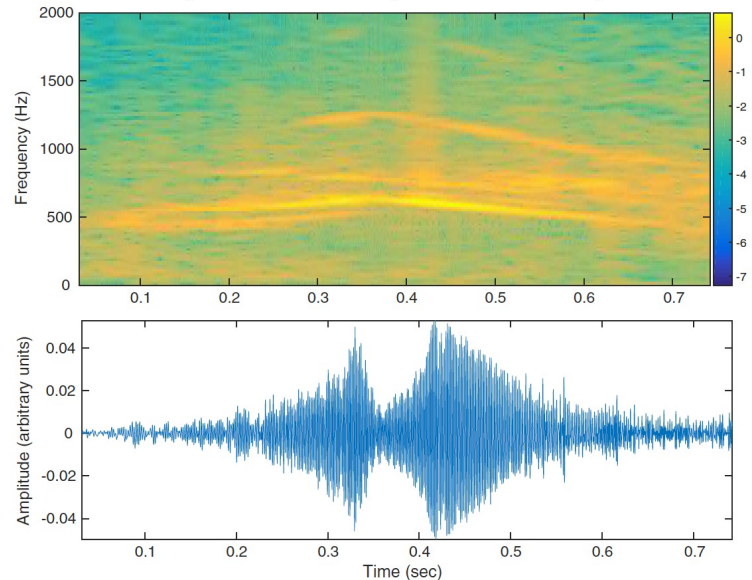
unmodeled chirps

- ▶ Chirp signal: $s(t) = a(t)\sin(\Phi(t))$,
 - ▶ Where the instantaneous frequency, $f(t) = \frac{d\Phi}{dt}$, changes adiabatically on timescales of the instantaneous period
 - ▶ \Rightarrow Track in the TF plane
- ▶ Unmodeled chirp signal: $a(t)$ and $f(t)$ have unknown functional forms



Unmodeled GW Chirps

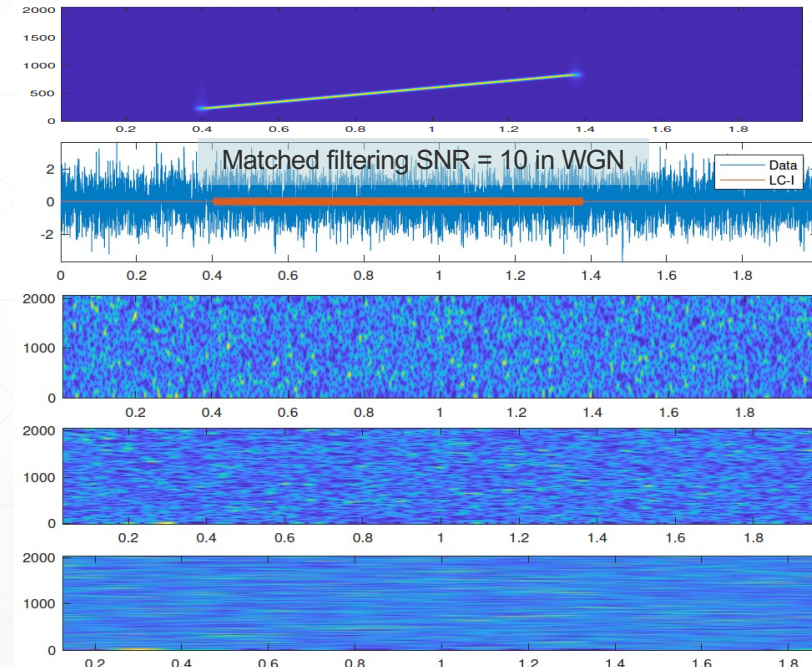
- All detected GW signals so far are chirps with theoretically predictable $a(t)$ and $f(t)$
- **Unmodeled** chirps: Either or both $a(t)$ and $f(t)$ are not well predicted by theory
- Post core-bounce phase of a core-collapse supernova [1,2]
- Dynamical instabilities in rotating newborn neutron stars [3,4]
- Clump formation or dynamical instabilities in the accretion disc surrounding a newly formed black hole in a collapsar [5,6]



1. Ott et al, Phys. Rev. Lett. 96, 201102 (2006).
2. Ott, Classical Quantum Gravity 26, 063001 (2009).
3. Liu, Phys. Rev. D 65, 124003 (2002).
4. Piro, Thrane, Astrophys. J. 761, 63 (2012).
5. van Putten, Phys. Rev. Lett. 87, 091101 (2001).
6. Kiuchi et al, Phys. Rev. Lett. 106, 251102 (2011).

Chirps: Detection and Estimation challenges

- ❖ Searches for unmodeled GW transient signals (“Bursts”) rely primarily on **time-frequency analysis**
- Chirps spread their energy along extended tracks in the time-frequency plane
- The consequent reduction in **local signal-to-noise ratio** makes their detection and estimation a challenge for time-frequency methods

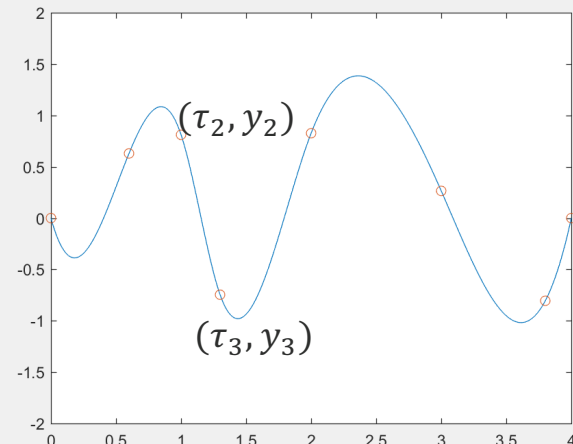


Search methods for GW chirps

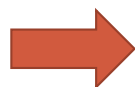
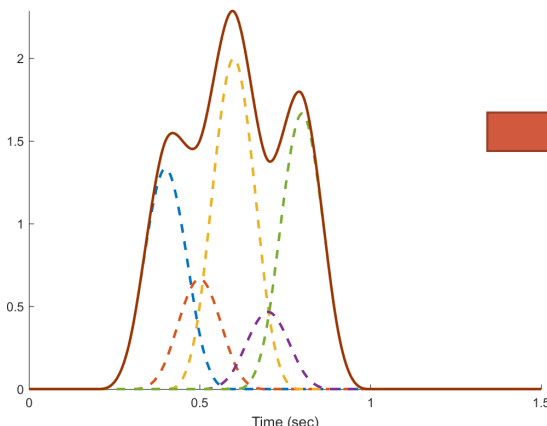
- TrackSearch: Image processing applied to Wigner-Ville (WV) time-frequency transform
 - W. G. Anderson and R. Balasubramanian, Phys. Rev. D 60, 102001 (1999).
- WV + sparsity regularization: Cleaning of non-linear artifacts
 - P. Addesso, M. Longo, S. Marano, V. Matta, I. Pinto, and M. Principe, in 2015 3rd International Workshop on Compressed Sensing Theory and its Applications to Radar, Sonar and Remote Sensing (CoSeRa) (IEEE, New York, 2015), p. 154.
- Beyond dependence on localized SNR in TF plane: The signal as a **chain of linear chirps** (piecewise linear approximation to $f(t)$);
 - Best Chirplet Chain: E. Chassande-Mottin and A. Pai, Phys. Rev. D 73, 042003 (2006).
 - Chirplet Path Pursuit: E. J. Candes, P. R. Charlton, and H. Helgason, Classical Quantum Gravity 25, 184020 (2008)

SEECR: Basic idea

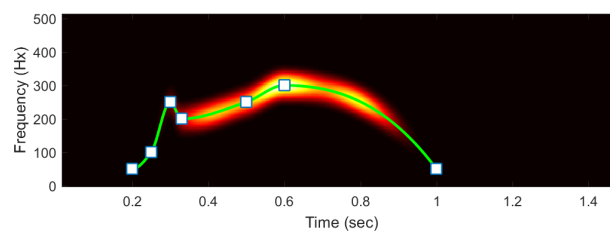
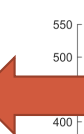
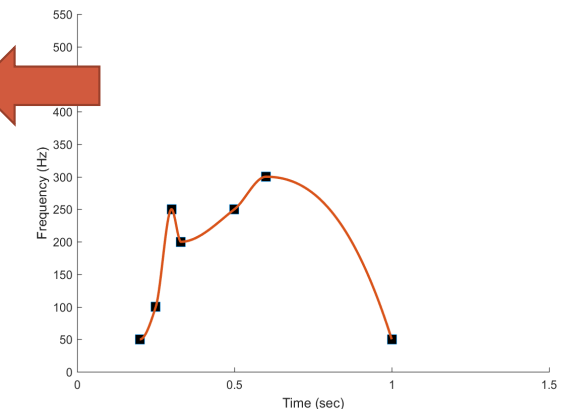
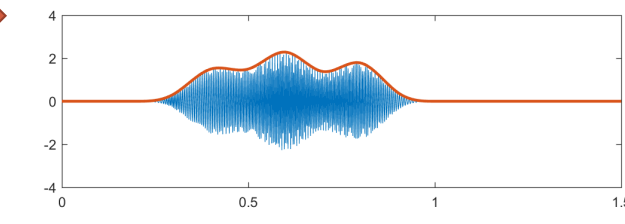
- Spline Enabled Effective-Chirp Regression
 - Mohanty, Phys Rev D, **96** 102008 (2017)
- Regularized least-squares fitting with model selection of a flexible chirp model
- Signal model: Both $a(t)$ and $f(t)$ are splines
- Refresher:
 - A spline is a piecewise polynomial function that interpolates $\{(\tau_i, y_i)\}; i = 0, 1, \dots, M - 1$
 - $\{\tau_0, \tau_1, \dots, \tau_{M-1}\}$: Set of knots
 - $\{y_0, y_1, \dots, y_{M-1}\}$: Set of data values at breakpoints



SEECR: Signal model



$$s(t) = a(t)\sin(\phi(t) + \phi_0)$$



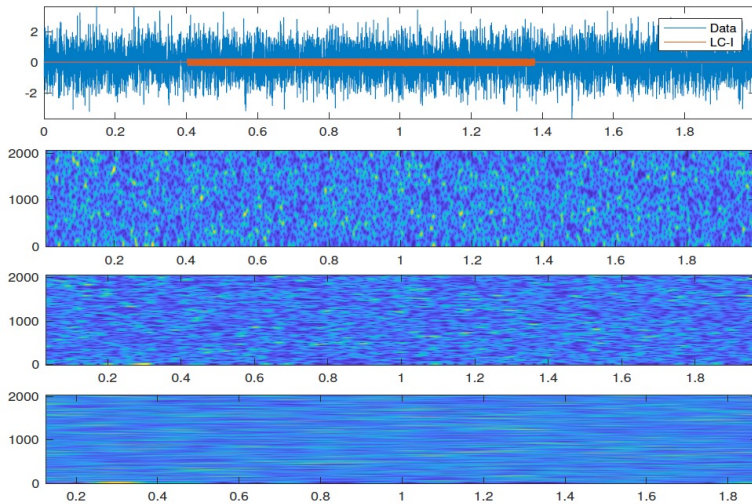
$$a(t) = \sum_{i=0}^{M-1} \alpha_i B_{i,k}(t)$$

$$\phi(t) = 2\pi \int_0^t f(t') dt'$$

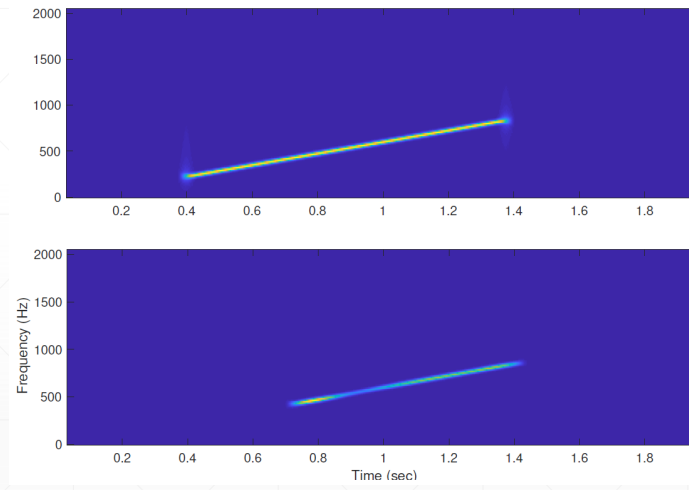
- Extrinsic parameters: amplitude spline and initial phase
- Intrinsic parameters: Time of arrival, frequency spline (knots and frequencies at knots)
- Very large number of intrinsic parameters (up to 14): PSO used for fitness optimization

SEECR Estimation performance: Examples

- Single data realization

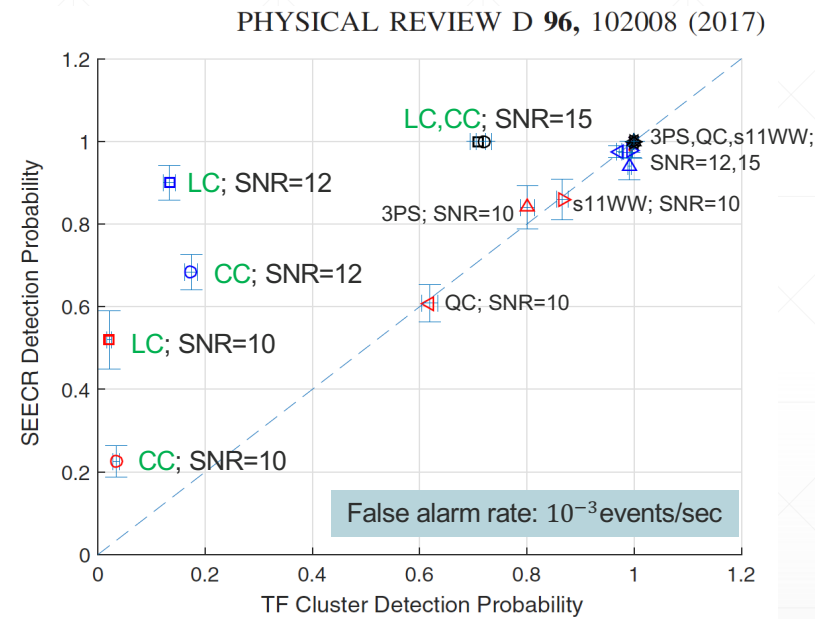


- True signal and SEECR estimate (spectrograms)



SEECR: Detection performance

- Tested across a wide range of chirp waveforms
 - White Gaussian Noise
 - Data length: 2sec sampled@4096Hz
 - 1 sec long Linear chirp with decreasing frequency (EUSIPCO paper)
- Significantly outperforms the sensitivity of a **multiresolution** time-frequency clustering method for some chirps; Not worse for others
- ❖ Time-frequency clustering is the main paradigm for current methods used for unmodeled GW searches
- ❖ Coherent WaveBurst; BayesWave



LC: Linear chirp (increasing frequency with time); 1sec long
CC: Cosine chirp; 1 sec
QC: Quadratic chirp; 1 sec

3PS: Strongly amplitude modulated sinusoid; 1.5 sec
s11WW: Acoustic supernova; 0.7 sec

HANDLING REAL GW DETECTOR NOISE

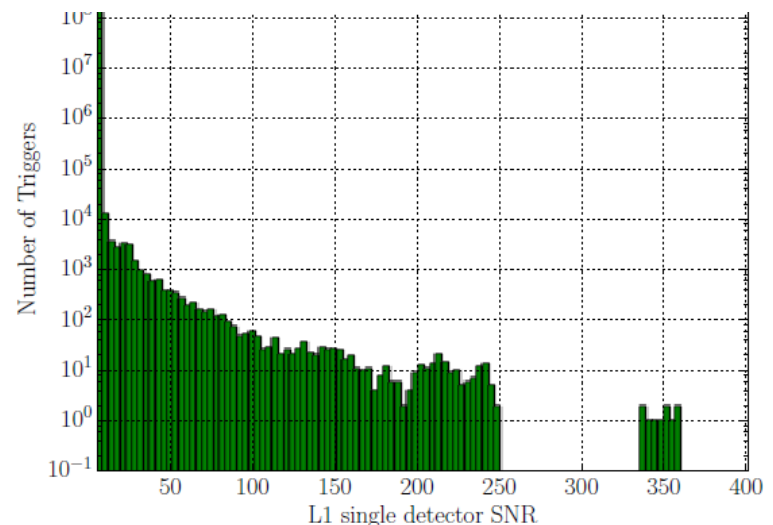
Vetoes

- GLRT/MLE assume a noise model
- The noise in real data never follows any noise model exactly: Instrumental artifacts, changing environment etc all contribute to deviations
- ⇒ A large number of events at the output of any GW search are not GW signals
- **Vetoes** are required to increase the rejection of spurious signals
 - Using **detector characterization** → Data quality vetoes
 - Using auxiliary channels
 - Using consistency tests
 - Example: χ^2 -veto in binary inspiral search
- Veto safety: We do not want too many GW signals to be removed accidentally
 - Hardware and software signal injections are needed to test safety

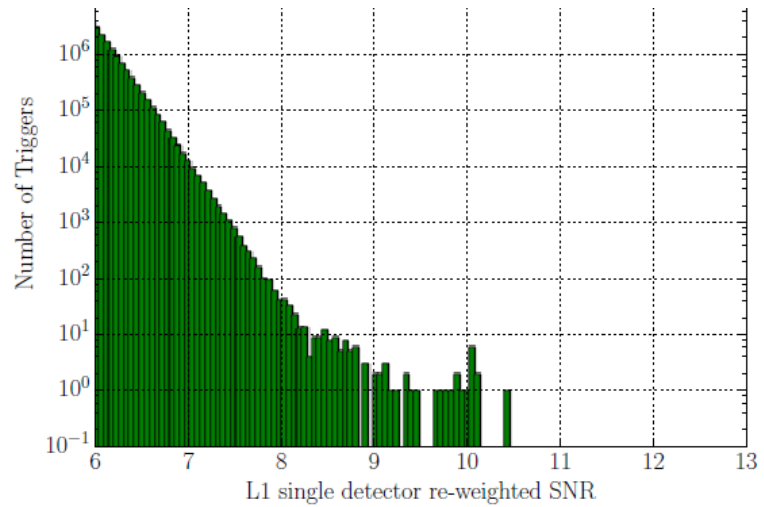
Effect of vetoes

arXiv:1710.02185v3 [gr-qc]

Histograms of single detector PyCBC triggers from the Livingston (L1) detector. These triggers were generated using data from September 12 to October 20, 2015. These histograms contain triggers from the entire [template bank](#), but exclude any triggers found in coincidence between the two detectors. (1a) A histogram of single detector triggers in SNR. The tail of this distribution extends beyond $\text{SNR} = 100$. (1b) A histogram of single detector triggers in re-weighted SNR. The [chi-squared test](#) down-weights the long tail of SNR triggers in the re-weighted SNR distribution. The triggers found using only the Hanford detector have a similar distribution.



(a)



Background rate estimation

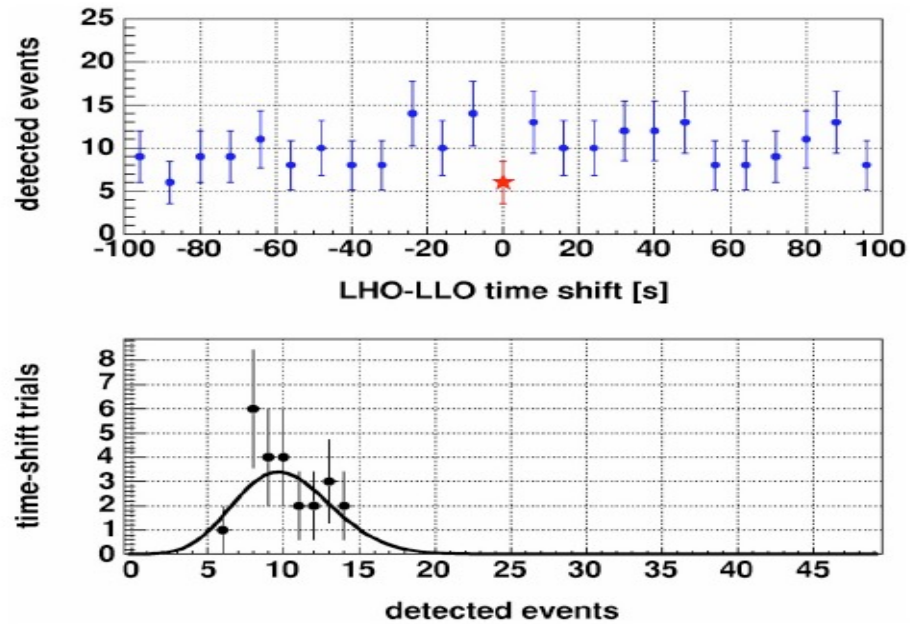
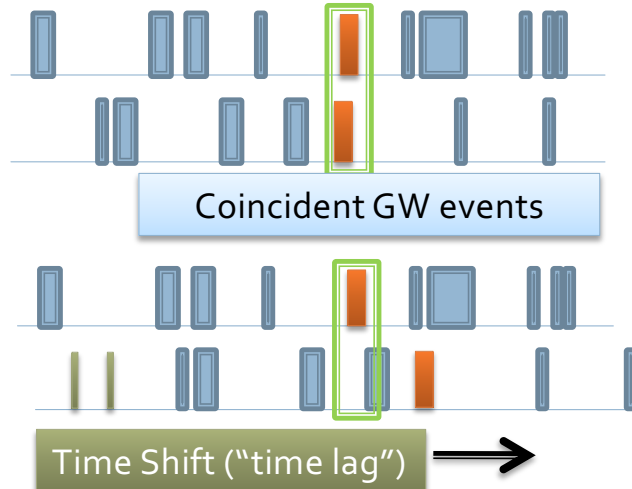
- Every GW detection must be accompanied by an estimated measure of our confidence that it is not a false alarm
- If the observed value of GLRT is $L_{G,obs}$: What is the expected rate of false alarms with $L_G \geq L_{G,obs}$?
- How can we measure small false alarm rates?
 - We do not have 50 years of noise to measure a rate of 1/50 years!
 - Real noise does not follow a Gaussian behavior, so we cannot calculate the rate theoretically

Name	Inst.	WB	GstLAL			MBTA					
			FAR (yr ⁻¹)	SNR	pastro	FAR (yr ⁻¹)	SNR	pastro	FAR (yr ⁻¹)	SNR	pastro
GW191103_012549	HL	—	—	—	—	—	—	—	27	9.0	0.13
GW191105_143521	HLV	—	—	—	24	10.0	0.07	0.14	10.7	> 0.99	
GW191109_010717	HL	< 0.0011	15.6	> 0.99	0.0010	15.8	> 0.99	1.8×10^{-4}	15.2	> 0.99	
GW191113_071753	HLV	—	—	—	—	—	—	26	9.2	0.68	
GW191126_115259	HL	—	—	—	80	8.7	0.02	59	8.5	0.30	
GW191127_050227	HLV	—	—	—	0.25	10.3	0.49	1.2	9.8	0.73	
GW191129_134029	HL	—	—	—	$< 1.0 \times 10^{-5}$	13.3	> 0.99	0.013	12.7	> 0.99	
GW191204_110529	HL	—	—	—	21	9.0	0.07	1.3×10^4	8.1	< 0.01	
GW191204_171526	HL	$< 8.7 \times 10^{-4}$	17.1	> 0.99	$< 1.0 \times 10^{-5}$	15.6	> 0.99	$< 1.0 \times 10^{-5}$	17.1	> 0.99	

- GWTC-3: Compact Binary Coalescences Observed by LIGO and Virgo During the Second Part of the Third Observing Run, arXiv:2111.03606
- (Additional entries from more pipelines in the table: not shown here)

Solution: artificial time-lags

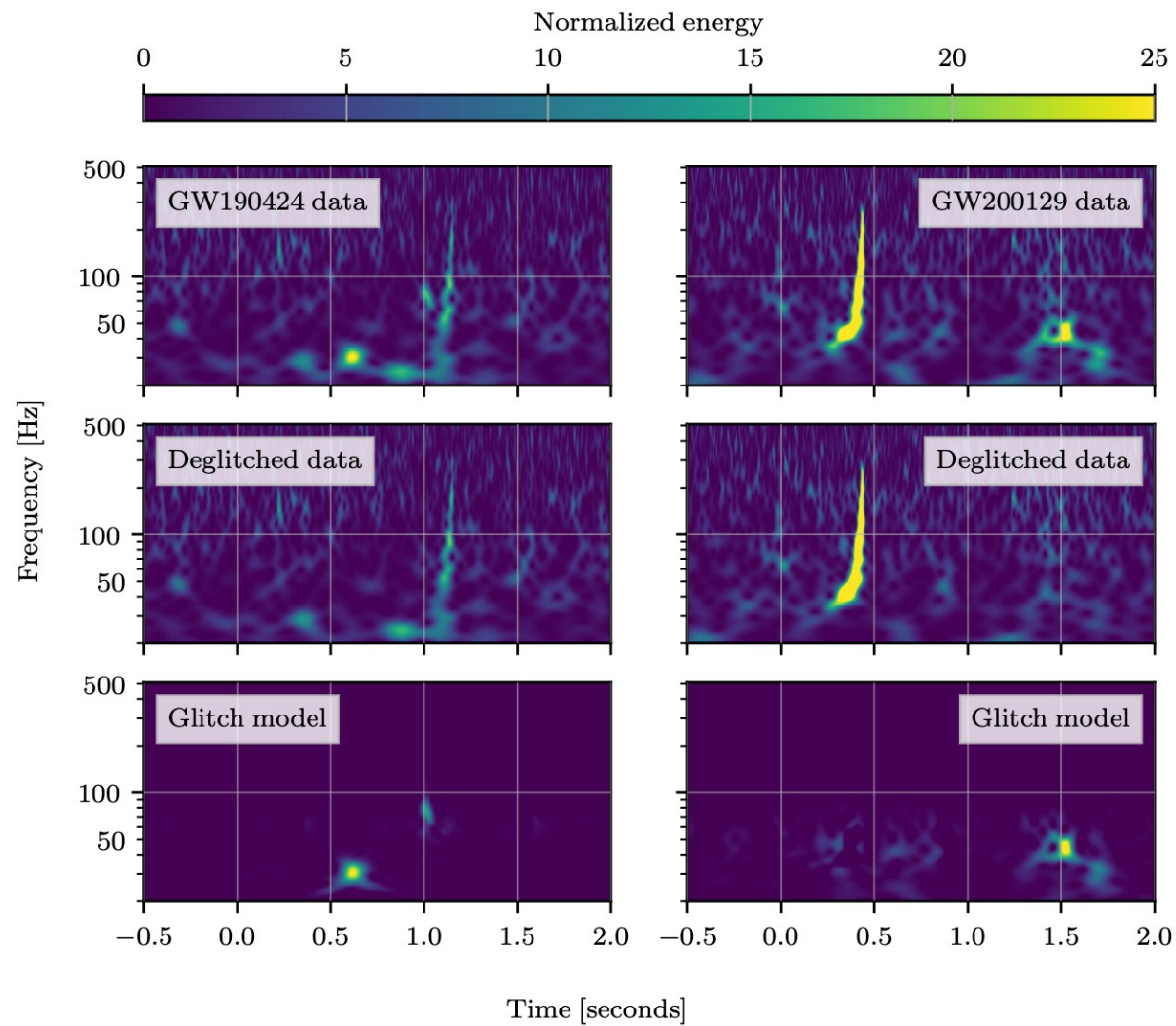
- Create new data sets where one detector's data is shifted in time relative to another by a large amount
- Re-analyze the new data sets using the same search method: All events must be coming from noise, not GWs
- Estimate false alarm rate (Assumption: shifted dataset are statistically independent)



- GW signals will not coincide in time-shifted data, so all observed coincidences are random
- Measure the number of coincidences for a set of time-lags
- Fit a poisson distribution and get rate

Glitch subtraction

- **Glitches:** short duration signals in GW strain data that are not GW signals: Instrumental and environmental artifacts
- *Subtracting glitches from gravitational-wave detector data during the third observing run*
D. Davis, T. B. Littenberg, I. M. Romero-Shaw, M. Millhouse, J. McIver, F. Di Renzo, G. Ashton
 - ... The high rate of these artifacts in turn results in a significant fraction of gravitational-wave signals from compact binary coalescences overlapping glitches. In LIGO-Virgo's third observing run, $\approx 20\%$ of signals required some form of mitigation due to glitches. This was the first observing run that glitch subtraction was included as a part of LIGO-Virgo-KAGRA data analysis methods for a large fraction of detected gravitational-wave events. This work describes the methods to identify glitches, the decision process for deciding if mitigation was necessary, and the two algorithms, BayesWave and gwssubtract, that were used to model and subtract glitches. Through case studies of two events, GW190424_180648 and GW200129_065458, we evaluate the effectiveness of the glitch subtraction, compare the statistical uncertainties in the relevant glitch models, and identify potential limitations in these glitch subtraction methods. We finally outline the lessons learned from this first-of-its-kind effort for future observing runs.

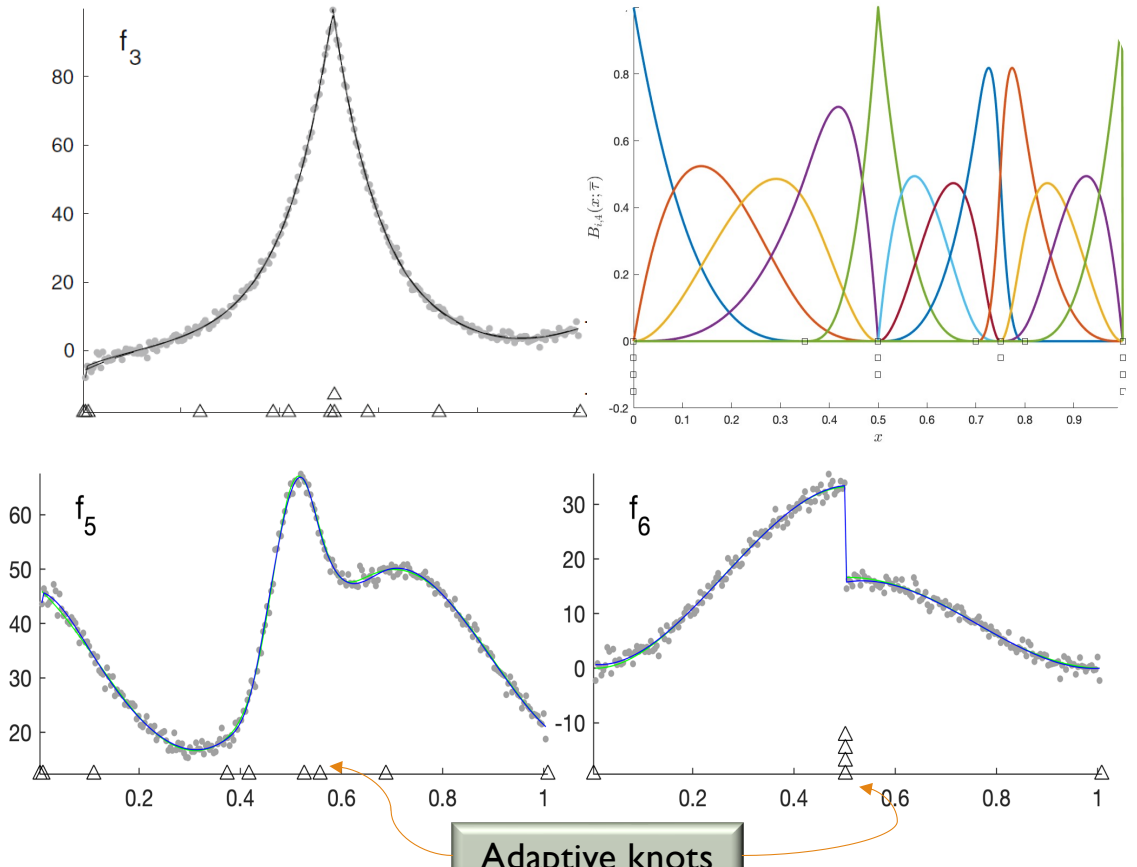


ADAPTIVE SPLINE

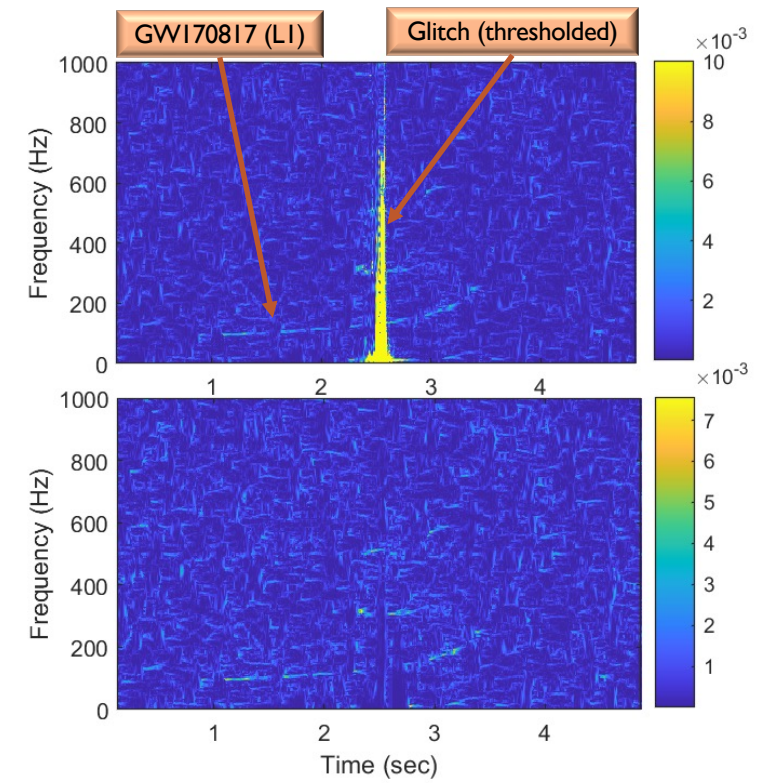
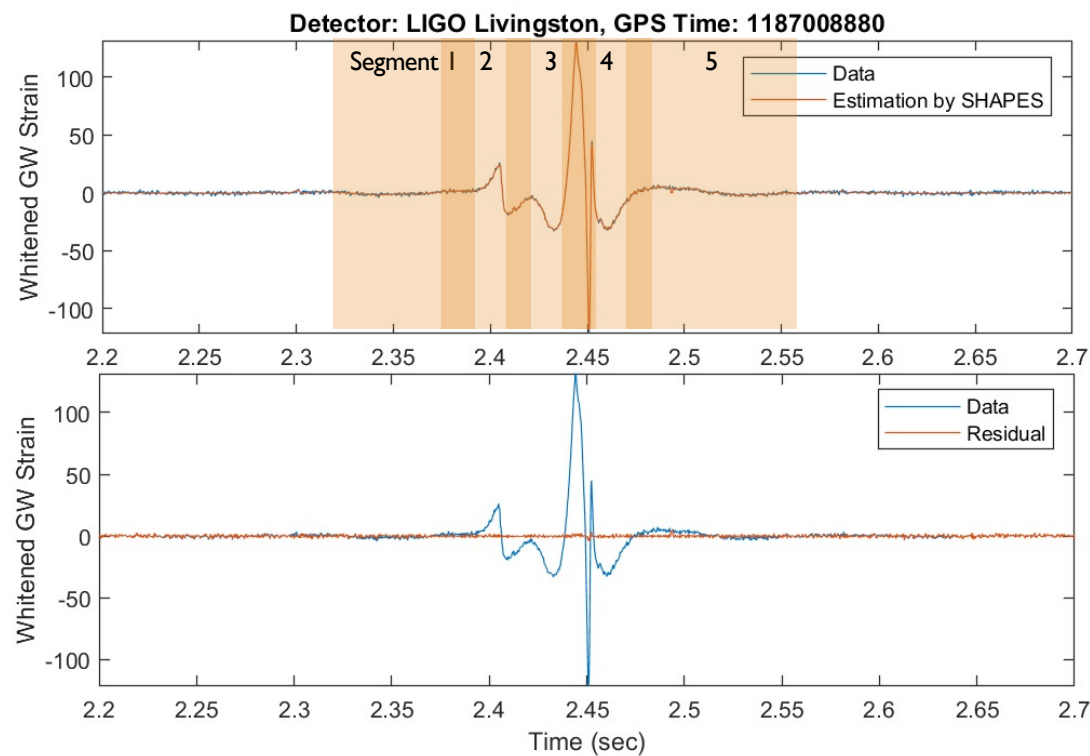
- **SHAPES:** Swarm Heuristics based Adaptive and Penalized Estimation of Splines
 - GitHub: mohanty-sd/SHAPES
 - Soumya D. Mohanty, E. Fahnestock, Computational Statistics (2020)
- Knots : $\bar{\tau} = (\tau_0, \tau_1, \dots, \tau_{P-1})$, $\tau_{i+1} \geq \tau_i$, $\tau_0 \geq 0$, $\tau_1 \leq 1$
- Any order k spline for the same $\bar{\tau}$ can be expressed as

$$f(x; \bar{\alpha}, \bar{\tau}) = \sum_{j=0}^{P-k-1} \alpha_j B_{j,k}(x; \bar{\tau})$$

- Estimated solution $\hat{f}(x; \hat{\alpha}, \hat{\tau})$
- $$(\hat{\alpha}, \hat{\tau}) = \min_{(\alpha, \tau)} \left[\sum_{i=0}^{N-1} (y_i - f(x_i; \bar{\alpha}, \bar{\tau}))^2 + \lambda \sum_{j=0}^{P-k-1} \alpha_j^2 \right]$$
- Optimization over $\bar{\tau}$ using PSO: ~ 20-dimensional space
 - Model selection using AIC over P

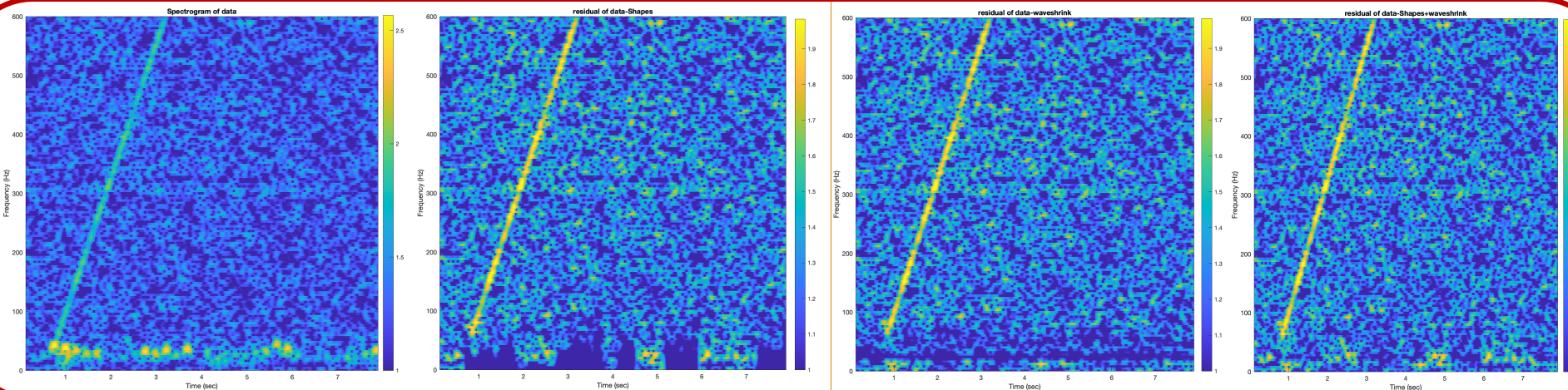


SHAPES: GLITCH SUBTRACTION



Adaptive spectrogram: Lukin, Todd, J. Audio Eng. Soc., 2006

GLITCH SUBTRACTION WITH ADAPTIVE SPLINE



SHAPES
Scooping of low frequency power

SHAPES + WaveShrink (Donoho & Johnstone, 1994)
Restoring low-frequency power

TOPICS NOT COVERED

- **Bayesian analysis:** The current trend in GW data analysis is to report Bayesian errors obtained using MCMC parameter estimation methods
- **Model selection**
 - Bayesian model selection: **Odds ratio**
 - Frequentist model selection: **Information criterion**
- **Machine learning applications in GW data analysis:** Classification of glitches
- **Cross-channel regression:** Removing noise in the GW strain time series using measurements from auxiliary sensors
- **Multisource resolution:** Future challenge for more sensitive GW detectors

Homework

Readings

- ▶ GWTC-3: Compact Binary Coalescences Observed by LIGO and Virgo During the Second Part of the Third Observing Run, arXiv:2111.03606
- ▶ Papers related to GW150914 and GW170817